Search for an Axionlike Spin Coupling Using a Paramagnetic Salt with a dc SQUID

Wei-Tou Ni, Sheau-shi Pan, Hsien-Chi Yeh, Li-Shing Hou, and Juling Wan
Center for Gravitation and Cosmology, Department of Physics, National Tsing Hua University, Hsinchu, Taiwan 30043, Republic of China
(Received 11 June 1998)

We use a paramagnetic salt TbF_3 with a dc SQUID to search for a possible axionlike $\boldsymbol{\sigma} \cdot \mathbf{r}$ interaction of a rotating copper mass with the salt. We set new limits on the axion coupling constant $g_s g_p/\hbar c$ and the finite-range Leitner–Okubo–Hari Dass coupling constant A. Our limit for range λ at 30 mm is 2 orders of magnitude better than previous results. For $\lambda > 30$ mm, $g_s g_p/\hbar c$ is $(0.14 \pm 0.67) \times 10^{-28}$, and A is less than 10. The outlook for further improvement is discussed. [S0031-9007(99)08656-1]

PACS numbers: 14.80.Mz, 04.80.Cc, 12.20.Fv, 13.10.+q

There are a number of groups experimentally searching for spin-dependent (semi-)long-range forces. These works are largely motivated to explore the role of spin in gravitation, and to explore the interaction associated with the exchange of a light or massless pseudoscalar Goldstone boson or similar interactions, e.g., arion interaction or axion interaction. Among the works to search for the spin-dependent (semi-)long-range forces, we can classify them into two categories: those searching for the monopole-dipole interactions [1–9] and those searching for the dipole-dipole interactions [5,10–17].

In connection with P (parity), and T (time reversal) noninvariance, Leitner and Okubo [18], and Hari Dass [19] suggested some time ago the following type of spin-gravity interaction,

$$H_{\text{int}} = f(r)\hat{\mathbf{r}} \cdot \boldsymbol{\sigma}, \tag{1}$$

where $\hat{\mathbf{r}}$ is the unit vector from the massive body to the particle with spin $\hbar\boldsymbol{\sigma}$. They assumed $f(r) = -AUm$ with U the gravitational potential of the massive body.

Fujii [20] proposed finite-range mass-mass interactions. More recently, Fischbach *et al.* proposed a fifth force which violates the equivalence principle with finite-range monopole-monopole interactions and stimulated many experimental efforts [21].

In our previous investigation [6], we used torsion balance with two cylindrical copper test masses and two cylindrical polarized "attracting" Dy_6Fe_{23} masses to search for finite-range mass-spin interactions with the Hamiltonian of the form (1). Our preliminary result showed that for the range of 3–5 cm, the upper limit of this interaction for our test mass and the Dy_6Fe_{23} polarized mass were below 1% of their gravitational interaction. We considered, in particular, the case of $f(r) = -Au^{-\mu r}mU$ with U the gravitational potential of the unpolarized body; that is, the finite-range mass-spin interaction is of the following form:

$$H_{\text{int}} = -Ae^{-\mu r}mU\hat{\mathbf{r}} \cdot \boldsymbol{\sigma}. \tag{2}$$

Ritter *et al.* [8], in a recent experiment, used spin-polarized Dy_6Fe_{23} masses acting on unpolarized copper masses in a dynamic-mode torsion pendulum and searched for the interaction of the axion [22–24] form,

$$H_{\text{int}} = [\hbar(g_s g_p)/8\pi mc](1/\lambda r + 1/r^2) \times \exp(-r/\lambda)\boldsymbol{\sigma} \cdot \hat{\mathbf{r}}. \tag{3}$$

In (3), λ is the range of the interaction, g_s and g_p are the coupling constants of vertices at the polarized and unpolarized particles, and m is the mass of the polarized particle. Constraints on the coupling $g_s g_p/\hbar c$ with respect to the range are plotted in a logarithmic plot (Fig. 1). For $\lambda < 0.3$ m, Refs. [6] and [8] give more stringent constraints than Refs. [5] and [7], and for $\lambda > 0.3$ m, vice versa. References [5] and [7] investigate the existence of hypothetical anomalous spin-dependent forces by sensing the interaction of polarized trapped ions with fermions in the Earth. These experiments are more sensitive to longer-range forces, while experiments with laboratory sources are more sensitive to shorter-range forces. Reference [9] has the best limit for $0.1 < \lambda < 8$ m. Our present work and our previous work [6] have the best limits for $\lambda < 0.1$ m.

Discovery and confirmation of the (13 ± 4) μK (5 ppm) quadrupole anisotropy in cosmic microwave

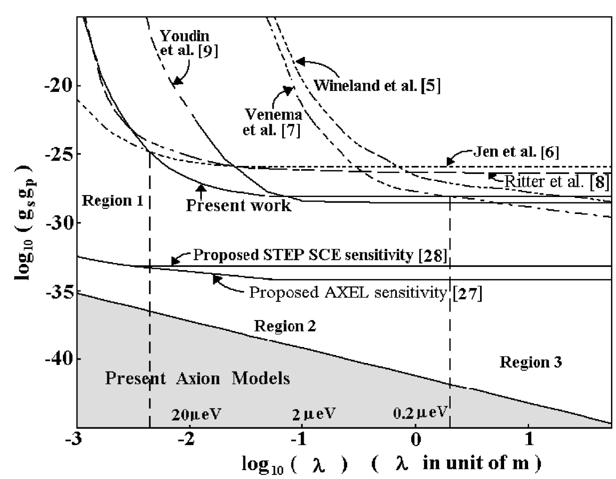

FIG. 1. Limits on $\boldsymbol{\sigma} \cdot \mathbf{r}$ spin coupling for axionlike interactions from various experiments.

background radiation favors cold dark matter cosmologies. Axions, other pseudoscalar Goldstone bosons, and neutrinos are possible candidates for cold dark matter. Microlensing observations suggest that brown dwarfs are not likely to be a major constitutent of dark matter, and searching for dark matter in the form of axions or other particles becomes even more critical. To search for this dark matter, it is important to experimentally determine the form of the interaction in the laboratory. Recent searches for axionic spin-dependent interactions are efforts in this direction. Experiments specifically searching for dark matter cosmic axion reach high sensitivity and a Kim-Shifman-Vainshtein-Zakharov axion of mass 2.9×10^{-6} to 3.3×10^{-6} eV is excluded as a dominant dark matter candidate in the halo of our Galaxy [25].

In an effort to solve the strong *CP* problem, axion theories were proposed [22,23]. In these theories, there are monopole-dipole interactions of the form (3), together with $\boldsymbol{\sigma} \cdot \boldsymbol{\sigma}$ (dipole-dipole) interactions. In Refs. [14–17], we searched for a dipole-dipole interaction and set experimental limits on the anomalous dipole-dipole interaction between electrons at $(1.2 \pm 2.0) \times 10^{-14}$ of the magnetic dipole interaction strength. Axionic monopole-dipole interaction has a larger magnitude than axionic dipole-dipole interaction. Here we search for this effect.

Vorobyov and Gitarts [11] first used induced ferromagnetism with a SQUID to search for spin-dependent forces. The Cooper pairs of the superconducting shields enclosing the SQUID detecting system provide magnetic shielding. The searched-for anomalous spin interaction due to an outside body would not be shielded by these Cooper pairs. This is a very clever idea. However, the ferromagnetic permeable material in their SQUID detector system was asked to be sensitive five-order beyond the actual test of these materials. To avoid this limiting factor, and to assure a clear understanding of a low-field response, we have used induced paramagnetism with a dc SQUID to search for spin-dependent forces [15–17]. In the present experiment, we follow our previous method. However, instead of polarized bodies, we use a copper cylinder as a mass source to search for finite-range mass-spin interactions [26]. With this simple external copper mass rotating around the superconducting shielded detector, a limit on the rotating magnetization of the paramagnetic salt TbF_3, as measured by our SQUID magnetometer, provides a more stringent test.

For a magnetic moment $\mathbf{m}$ in a magnetic field $\mathbf{B}$, the Hamiltonian is $H_{\text{mag}} = -\mathbf{m} \cdot \mathbf{B}$, with $\mathbf{m} = \mu_e \boldsymbol{\sigma}$ for the electron. Compared with (1), the anomalous monopole-spin interaction on an electron is equivalent to a $\mathbf{B}$ field of

$$\mathbf{B}_{\text{eff}} = -(1/\mu_e) f(r) \hat{\mathbf{r}} . \qquad (4)$$

For axion interaction,

$$\mathbf{B}_{\text{eff}} = -\frac{\hbar}{\mu_e} \frac{g_s g_p}{8\pi m_e c} \left(\frac{1}{\lambda r} + \frac{1}{r^2} \right) \exp(-r/\lambda) \hat{\mathbf{r}} , \qquad (5)$$

for the field generated by a nucleon on an electron. For the field generated by copper mass, an integration over the copper mass is needed.

In this experiment, we sensitively measure the possible $\mathbf{B}_{\text{eff}}$ field. The scheme of our experimental setup is shown in Fig. 2. The paramagnetic salt and SQUID detection system is the same as in Refs. [15–17]. The various parts are described below.

The paramagnetic salt.—We use a terbium fluoride cylinder of 0.462 cm diameter and length 1.19 cm. Terbium fluoride has a ferromagnetic phase transition temperature T_c of 3.95 K. Its susceptibility is measured using an rf SQUID magnetometer to be $\chi = 0.16$ at 4.2 K, i.e., $\mu = 1 + 4\pi\chi = 3.01$.

The magnetism of the terbium fluoride comes from the terbium ion which has $S = 3$, $L = 3$, and $J = 6$. About two thirds of the magnetic moment of the terbium ion come from its spin. Hence the χ for the spin magnetism is two thirds of the value measured for the total angular momentum.

The copper cylinder.—Our copper mass is a 25.41 mm o.d. cylinder with a thickness of 54.14 mm and a mass M of 976.3 g. The center-to-center distance of the copper mass and the paramagnetic salt is 57.1 mm.

dc SQUID system and the magnetic shields.—A low noise dc SQUID system with a noise specification of $5 \times 10^{-6} \phi_0/\sqrt{\text{Hz}}$ ($\phi_0 = 2.0678 \times 10^{-7}$ G cm^2 is the magnetic flux quantum) is connected to a superconducting pickup loop coupled to the salt. Any changes in the magnetization are detected as the copper cylinder is rotated outside the Dewar, but separated from the TbF_3 sample by one μ-metal shield at room temperature and two niobium superconducting shields at 4.2 K. The

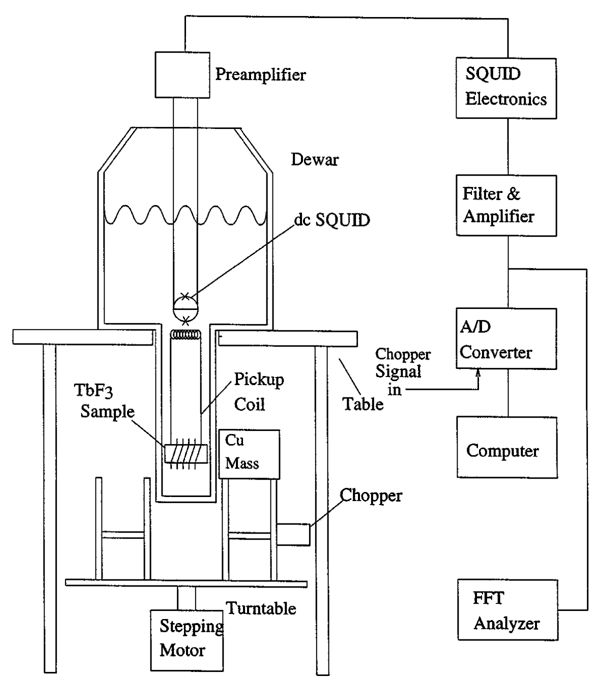

FIG. 2. Schematic for spin-coupling experiment.

magnetic field is shielded by the superconducting electric current, while the effective field associated with the copper cylinder is unaffected. The magnetic field inside the μ-metal shield for the Dewar is typically 1–2 mG or lower. The two niobium superconducting shields give a shielding factor better than 10^{10}. The Earth and environmental magnetic shield is less than 0.5 G.

Pickup coil and SQUID sensitivity.—The pickup coil and SQUID sensitivity to the magnetic field is calibrated in our previous measurement [15–17] to be $46\,550\phi_0\ \mathrm{G}^{-1}$ without the TbF_3 paramagnetic salt. With this salt in the pickup coil, the additional increase in the dc SQUID response is $66\,500\phi_0\ \mathrm{G}^{-1}$. Since two thirds of the magnetization of the salt are due to the spin of TbF_3 and only intrinsic spins are responsive to the effective $\mathbf{B}_{\mathrm{eff}}$ field, the sensitivity to the $\mathbf{B}_{\mathrm{eff}}$ field is two thirds of the above values, i.e., $43\,500\phi_0\ \mathrm{G}^{-1}$.

Measurement procedure.—As in Fig. 2, the copper mass is sitting on one side of the turntable underneath the Dewar. In the data taking, a laser beam and a chopper-photodetector system is used to lock the output signal of the dc SQUID to the rotation angle of the polarized bodies. The laser beam is intercepted by the chopper when the copper axis is in line with the axis of the paramagnetic salt. We define this angle to be zero degrees, and expect the $\boldsymbol{\sigma} \cdot \mathbf{r}$ interaction signal to be proportional to $\cos\Theta$, where Θ is the angular position of the copper mass.

To start the measurement, we set the turntable with the copper mass rotating at 0.96 c/s with a stepping motor system. The stability of the rotation speed is better than 10^{-4}. The output of voltage of the dc SQUID system for $1\phi_0$ from the most sensitive scale of the dc SQUID controller is 10 V. This output is further amplified 1000 times and low-pass filtered to a 10 Hz bandwidth, and then read into a computer with an analog-to-digital converter (ADC). The angular position of the copper mass is simultaneously read into this computer. The typical noise of the SQUID output after 1000 times amplification and 10 Hz low-pass filtering as recorded by ADC is about ± 300 mV. This is consistent with the dc SQUID noise of $200\ \mathrm{mV}/\sqrt{\mathrm{Hz}}$ after amplification. When we average the data for 400 cycles, the typical output is about ± 50 mV and the pattern repeats. To subtract this interference background, we average the data for 4–5 h, alternatively take away and put back the copper cylinder to average the data for another 4–5 h, and subtract the results to find the net effects.

Results and analysis.—The top of Fig. 3 shows the results of a typical run. The curve with open circles shows the result for the configuration of Fig. 2; the curve with crosses shows the result with the copper mass removed. Their difference is shown as the third curve. We Fourier transform this third curve to find the sine, cosine, and total amplitudes of the fundamental frequency (0.96 c/s) and different harmonics. The total amplitudes are shown in the bottom of Fig. 3. The 10 Hz filtering effect is clear. This $\sin\Theta$ and $\cos\Theta$ amplitudes of fundamental frequency are 6.63 and 1.1 mV, respectively. Table I lists the results of six runs. The last column lists the total Fourier amplitude corresponding to the fundamental frequency. We use this amplitude as our uncertainty measure. The weighted average of the six runs for the amplitude of the $\cos\Theta$ component is (0.49 ± 2.34) mV. Expressed in terms of flux amplitude, it becomes $(0.49 \pm 2.34) \times 10^{-7}\phi_0$. Converted to $\mathbf{B}_{\mathrm{eff}}$, we have $(1.13 \pm 5.38) \times 10^{-12}$ G. Using the integral version of (5), the coupling constant $g_s g_p/\hbar c$ is $(0.14 \pm 0.67) \times 10^{-28}$ for $\lambda > 30$ mm. Our experimental constraint on the coupling constant $g_s g_p/\hbar c$

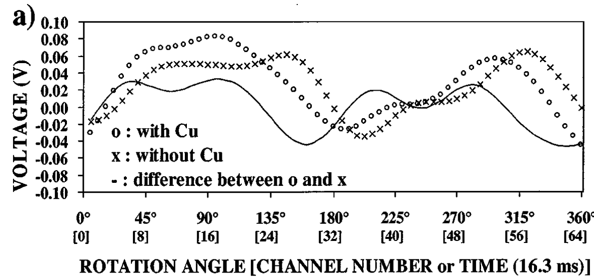

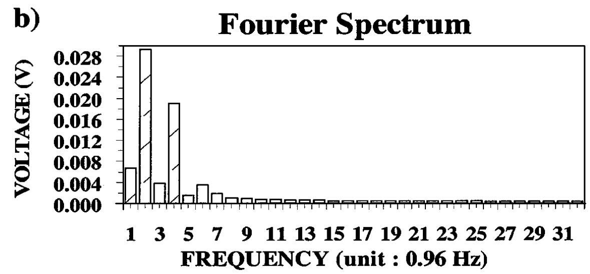

FIG. 3. (a) Multichannel average of a typical run for the dc SQUID output, amplified 1000 times with 10 Hz low-pass filtering. The ordinate shows the voltage output. 1 V output $(10^{-4}\phi_0)$ corresponds to 2.3×10^{-9} G in the effective field $\mathbf{B}_{\mathrm{eff}}$. The absissa shows the rotation angle of the copper mass with corresponding channel number or time (with unit 16.3 ms). The curve with open circles shows the results with the copper mass on as in the configuration of Fig. 2; the curve with crosses shows the results with the copper mass removed. Their difference is shown as the third curve. (b) Fourier spectrum of the difference curve in (a). The ordinate shows the amplitude derived from the Fourier sine and cosine transforms of the time sequence. The absissa shows the corresponding frequency. Note that the 10 Hz filtering is apparent in this diagram.

TABLE I. Fourier amplitudes of the fundamental frequency (0.96 Hz) of six runs to search for spin-dependent forces.

Run No.	$\sin\Theta$ amplitude (mV)	$\cos\Theta$ amplitude (mV)	Total amplitude (mV)
1	2.12	−2.33	3.15
2	1.4	11.87	11.95
3	−3.91	6.5	7.57
4	−5.57	−0.58	5.6
5	−4.7	−16.1	16.8
6	6.63	1.1	6.72

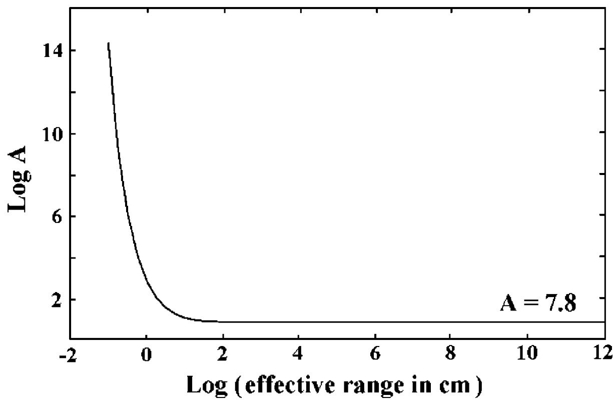

FIG. 4. Experimental constraints on the finite-range Leitner–Okubo–Hari Dass interaction from the present experiment.

improves the previous results by 2 orders of magnitude at $\lambda = 30$ mm. Further improvement will be implemented.

The allowed parameter region for the theoretical model represented by Eq. (2) is the region below the curve in Fig. 4. For $\lambda = \mu^{-1} > 30$ mm, A is less than 10.

Outlook.—We are currently improving on the sensitivity of this experiment. With array (multiple-sensor) configuration ($V_d \approx 10^{-3}$ m^3), dense mass, magnetization-noise-limited performance, and longer integration time (one year), the sensitivity would be enhanced by more than 5 orders of magnitude. The sensitivity of this proposal—AXEL (axial experiment at low temperature) [27] is shown in Fig. 1.

As shown in Fig. 1, the STEP spin-coupling experiment [28] proposes to search for any coupling force between spin-polarized and ordinary matter to a sensitivity of $g_s g_p/\hbar c = 6 \times 10^{-34}$ at a range of 1 mm or longer. So is the AXEL spin-coupling experiment.

Speake's group at the University of Birmingham is working on the development of a new superconducting torsion balance to detect force on the mass for the spin-coupling experiment. H. J. Paik at the University of Maryland proposes to use superconducting accelerometers for a spin-coupling experiment with a high Q. They are also aiming at very significant improvement.

With 5 orders of magnitude improvement, sensitivity of 10^{-33} in the axion coupling constant $g_s g_p/\hbar c$ and sensitivity of 10^{-4} in the finite-range Leitner–Okubo–Hari Dass coupling constant A at a range of 1 mm or longer can be achieved. Spin-coupling experiments and dark matter axion search experiments complement themselves in the long run in the search for new interactions and a new form of matter.

We thank Riley Newman for discussion on the comparisons of various $\boldsymbol{\sigma} \cdot \mathbf{r}$ experiments. This work is supported in part by the National Science Council of the Republic of China.

[1] C.-H. Hsieh *et al.,* Mod. Phys. Lett. A **4**, 1597 (1989).
[2] W.-T. Ni, Physica (Amsterdam) **165B & 166B**, 157 (1990).
[3] Y. Chou *et al.,* Mod. Phys. Lett. A **5**, 2297 (1990).
[4] J. M. Daniels and W.-T. Ni, Mod. Phys. Lett. A **6**, 659 (1991).
[5] D. J. Wineland *et al.,* Phys. Rev. Lett. **67**, 1735 (1991).
[6] T.-H. Jen *et al.,* in *Proceedings of the Sixth Marcel Grossmann Meeting on General Relativity,* edited by H. Sato and T. Nakamura (World Scientific, Singapore, 1992), pp. 489–494.
[7] B. J. Venema *et al.,* Phys. Rev. Lett. **68**, 135 (1992).
[8] R. C. Ritter *et al.,* Phys. Rev. Lett. **70**, 701 (1993). The limit on the electron has been multiplied by $8\pi^2$ to be consistent with our notation [R. C. Ritter (private communication)].
[9] A. N. Youdin *et al.,* Phys. Rev. Lett. **77**, 2170 (1996).
[10] D. Graham and R. Newman, in *Proceedings of the Eleventh International Conference on General Relativity and Gravitation, Stockholm, Sweden, 1986,* edited by M. A. H. MacCallum (Cambridge University Press, New York, 1987), p. 614; D. Graham, Ph.D. thesis, University of California, Irvine, 1987.
[11] P. V. Vorobyov and Ya. I. Gitarts, Phys. Lett. B **208**, 146 (1988).
[12] R. C. Ritter *et al.,* Phys. Rev. D **42**, 977 (1990).
[13] V. F. Bobrakov *et al.,* Pis'ma Zh. Eksp. Teor. Fiz. **53**, 283 (1991) [JETP Lett. **53**, 294 (1991)].
[14] S.-s. Pan *et al.,* Mod. Phys. Lett. A **7**, 1287 (1992).
[15] T. C. P. Chui and W.-T. Ni, Phys. Rev. Lett. **71**, 3247 (1993).
[16] W.-T. Ni *et al.,* Int. J. Mod. Phys. **8**, 5153 (1993).
[17] W.-T. Ni *et al.,* Physica (Amsterdam) **194B–196B**, 153 (1994).
[18] J. Leitner and S. Okubo, Phys. Rev. **136**, B1542 (1964).
[19] N. D. Hari Dass, Phys. Rev. Lett. **36**, 393 (1976); Ann. Phys. (N.Y.) **107**, 337 (1977).
[20] Y. Fujii, Ann. Phys. (N.Y.) **69**, 494 (1972); Nature Phys. Sci. **234**, 5 (1971).
[21] E. Fischbach *et al.,* Phys. Rev. Lett. **56**, 3 (1986); E. Fischbach and C. Talmadge, Mod. Phys. Lett. A **4**, 2303 (1989); E. G. Adelberger *et al.,* Phys. Rev. D **42**, 3267 (1990); Y. Fujii, Mod. Phys. A **6**, 3505 (1991).
[22] S. Weinberg, Phys. Rev. Lett. **40**, 233 (1978); F. Wilczek, Phys. Rev. Lett. **40**, 279 (1978); M. Dine *et al.,* Phys. Lett. **104B**, 1999 (1981); M. Shifman *et al.,* Nucl. Phys. **B166**, 493 (1980); J. Kim, Phys. Rev. Lett. **43**, 103 (1979).
[23] S.-L. Cheng *et al.,* Phys. Rev. D **52**, 3132 (1995), and references therein.
[24] J. E. Moody and F. Wilczek, Phys. Rev. D **30**, 130 (1984).
[25] C. Hagmann *et al.,* Phys. Rev. Lett. **80**, 2043 (1998), and references therein.
[26] Preliminary result reported in W.-T. Ni *et al.,* in *Proceedings of Seventh Marcel Grossmann Meeting on General Relativity* (World Scientific, Singapore, 1996), p. 1625.
[27] W.-T. Ni, Classical Quantum Gravity **13**, A135 (1996); W.-T. Ni, in the CD-ROM *Proceedings for the International Workshop on Gravitation and Astrophysics, Tokyo, 1997* (ICRR, Tokyo, 1998).
[28] D. Shaul *et al.,* Classical Quantum Gravity **13**, A107 (1996), and references therein.